




Article

Monteneroite, $\text{Cu}^{2+}\text{Mn}_2^{2+}(\text{AsO}_4)_2 \cdot 8\text{H}_2\text{O}$, a new vivianite-structure mineral with ordered cations from the Monte Nero mine, Liguria, Italy

Anthony R. Kampf^{1*} , Jakub Plášil², Barbara P. Nash³, Marco E. Ciriotti^{4,5}, Fabrizio Castellarò⁶ and Luigi Chiappino⁷

¹Mineral Sciences Department, Natural History Museum of Los Angeles County, 900 Exposition Boulevard, Los Angeles, CA 90007, USA; ²Institute of Physics ASCR, v.v.i., Na Slovance 1999/2, 18221 Prague 8, Czech Republic; ³Department of Geology and Geophysics, University of Utah, Salt Lake City, Utah 84112, USA; ⁴Associazione Micromineralogica Italiana, via San Pietro 55, I-10073 Devesi-Cirié, Torino, Italy; ⁵Dipartimento di Scienze della Terra, Università degli Studi di Torino, via Tommaso Valperga Caluso 35, I-10125 Torino, Italy; ⁶via XXV Aprile 28, I-16046 Mezzanago, Italy; and ⁷via Palmanova 67, I-20132 Milano, Italy

Abstract

Monteneroite (IMA2020-028), $\text{Cu}^{2+}\text{Mn}_2^{2+}(\text{AsO}_4)_2 \cdot 8\text{H}_2\text{O}$, is a new vivianite-structure mineral from the Monte Nero mine, Rocchetta di Vara, La Spezia, Liguria, Italy. It is a secondary mineral that crystallised from As-, Cu- and Mn-rich fluids and it is associated with braunite, copper, cuprite, rhodochrosite and strashimirite. Monteneroite occurs as light green, thick blades up to ~2.5 mm long. The streak is white. Crystals are transparent with vitreous lustre. The mineral has Mohs hardness of 2, is somewhat sectile, exhibits two cleavages ($\{010\}$ perfect and $\{001\}$ fair) and has irregular stepped fracture. The measured density is $2.97(2) \text{ g cm}^{-3}$. Monteneroite is optically biaxial (+), with $\alpha = 1.604(2)$, $\beta = 1.637(2)$ and $\gamma = 1.688(2)$, determined in white light; $2V = 80(1)^\circ$; slight dispersion is $r < v$, orientation: $X = \mathbf{b}$; $Z \wedge c = 52^\circ$ in obtuse β . Electron microprobe analyses provided the empirical formula $(\text{Cu}_{0.88}\text{Mn}_{0.11})_{\Sigma 0.99}\text{Mn}_{2.00}^{2+}(\text{As}_{1.00}\text{O}_4)_2 \cdot 8\text{H}_2\text{O}$. Monteneroite is monoclinic, $C2/m$, $a = 10.3673(14)$, $b = 13.713(2)$, $c = 4.8420(8) \text{ \AA}$, $\beta = 105.992(8)^\circ$, $V = 661.72(18) \text{ \AA}^3$ and $Z = 2$. Monteneroite has a vivianite-type structure ($R_1 = 0.0535$ for 534 $I > 2\sigma I$ reflections). It is the first mineral with this structure type to be defined with ordered octahedral cation sites.

Keywords: monteneroite, new mineral, crystal structure, Raman spectroscopy, vivianite structure type, Monte Nero mine, Liguria, Italy

(Received 17 July 2020; accepted 22 September 2020; Accepted Manuscript published online: 28 September 2020; Associate Editor: David Hibbs)

Introduction

Phases with the vivianite structure type have the general structural formula $M1M2_2(\text{TO}_4)_2 \cdot 8\text{H}_2\text{O}$, where $M1$ and $M2$ are divalent cations (Mg, Mn, Fe, Co, Ni, Cu and Zn) in two symmetrically distinct, octahedrally coordinated sites and T is a tetrahedrally coordinated cation (P or As). To date, four phosphate minerals and seven arsenate minerals have been described with the vivianite structure. Until now, all minerals and synthetic vivianite-type phases, except baričite, have exhibited dominance of the same cation in the $M1$ and $M2$ sites, although partial ordering has been documented in some cases. The reader is referred to the detailed discussion of this subject in the descriptive paper on babánekite, $\text{Cu}_3(\text{AsO}_4)_2 \cdot 8\text{H}_2\text{O}$, by Plášil *et al.* (2017). Note that Yakubovich *et al.* (2001) showed Fe to be dominant in the $M1$ site and Mg to be dominant in the $M2$ site in baričite; however, the mineral has never been formally redefined to reflect this and it is still regarded as the Mg-dominant analogue of vivianite with the formula $(\text{Mg,Fe})_3(\text{PO}_4)_2 \cdot 8\text{H}_2\text{O}$. The new mineral monteneroite, $\text{Cu}^{2+}\text{Mn}_2^{2+}(\text{AsO}_4)_2 \cdot 8\text{H}_2\text{O}$, described herein, is the first mineral

with the vivianite structure to be formally defined on the basis of the dominance of different cations in the $M1$ and $M2$ sites. We are convinced that, besides monteneroite and baričite, other vivianite-structure-type phases with ordered cations exist. We intend to conduct structural investigations of other likely candidates with the purpose of formally establishing the vivianite group with cation dominance in the $M1$ and $M2$ sites considered separately.

The new mineral monteneroite is named for its type locality, the abandoned Monte Nero mine in Liguria, Italy. The new mineral and name have been approved by the Commission on New Minerals, Nomenclature and Classification of the International Mineralogical Association (IMA2020-028, Kampf *et al.*, 2020). One holotype specimen is deposited in the Natural History Museum of Los Angeles County, Los Angeles, California, USA, under catalogue number 67509.

Occurrence

Monteneroite was discovered by Fabrizio Castellarò on a single small specimen collected from the ‘classic’ dump at the Monte Nero mine, Rocchetta di Vara, La Spezia, Liguria, Italy ($44^\circ 14'48''\text{N}$, $9^\circ45'27''\text{E}$). The deposit is comprised of thin manganese stratiform ores that are located near the base of a chert sequence in the ‘Diaspri di Monte Alpe’ formation, which overlays Jurassic

*Author for correspondence: Anthony R. Kampf, Email: akampf@nhm.org

Cite this article: Kampf A.R., Plášil J., Nash B.P., Ciriotti M.E., Castellarò F. and Chiappino L. (2020) Monteneroite, $\text{Cu}^{2+}\text{Mn}_2^{2+}(\text{AsO}_4)_2 \cdot 8\text{H}_2\text{O}$, a new vivianite-structure mineral with ordered cations from the Monte Nero mine, Liguria, Italy. *Mineralogical Magazine* 84, 881–887. <https://doi.org/10.1180/mgm.2020.76>

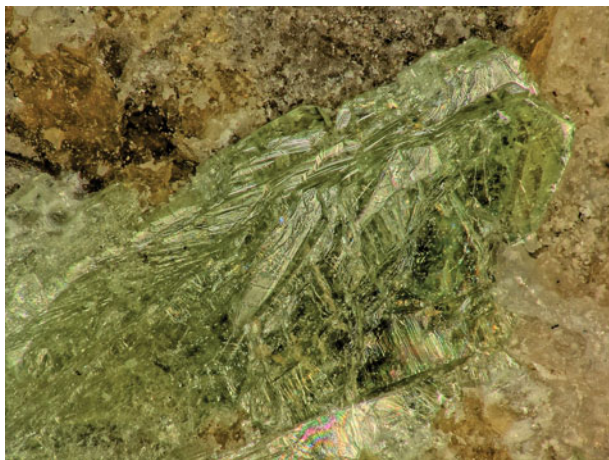


Fig. 1. Intergrown blades of monteneroite on the holotype specimen; field of view: 1.8 mm across (Natural History Museum of Los Angeles County, catalogue number 67509).

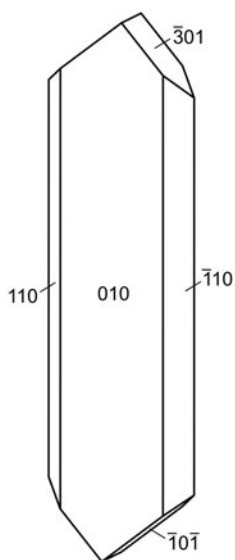


Fig. 2. Crystal drawing of monteneroite; clinographic projection in nonstandard orientation.

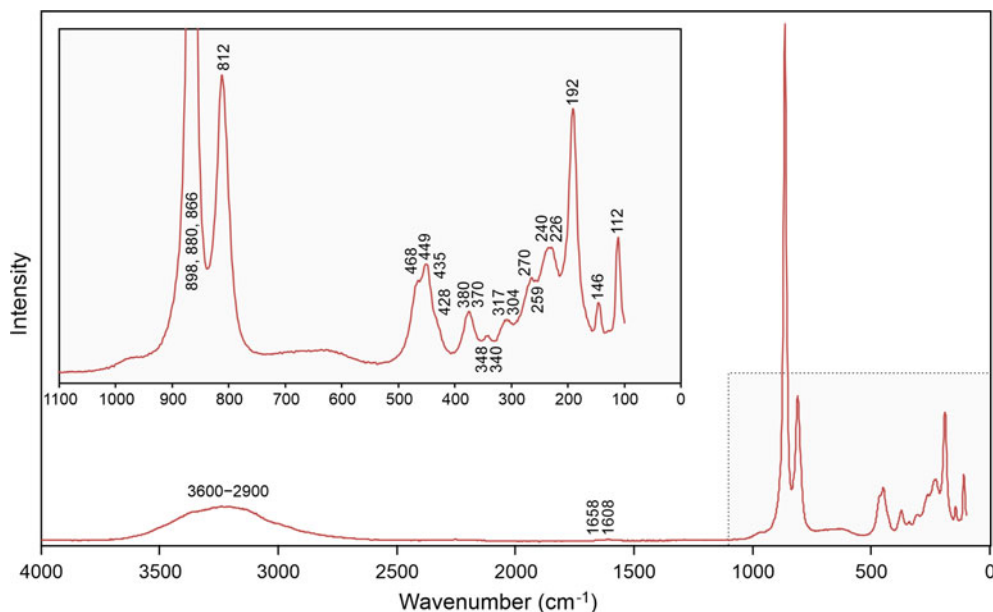


Fig. 3. Raman spectrum of monteneroite.

ophiolites of the Bracco unit. Monteneroite is a secondary mineral that crystallized from As-, Cu- and Mn-rich fluids, which circulated through a system of fractures during the final tectono-metamorphic stage of the deposit (Marescotti and Cabella, 1996). Other minerals found with monteneroite include braunite, copper, cuprite, rhodochrosite and strashimirite. The Monte Nero mine is also the type locality for coralloite (Callegari *et al.*, 2012) and castellaroite (Kampf *et al.*, 2016). More information on the deposit can be found in Callegari *et al.* (2012) and references therein.

Physical and optical properties

Monteneroite occurs as light green, thick blades up to ~ 2.5 mm long (Fig. 1). Blades are elongated on $[001]$ and flattened on $\{010\}$ and exhibit the forms $\{010\}$, $\{110\}$, $\{101\}$ and $\{30\bar{1}\}$ (Fig. 2). Note that it was impractical to measure the forms; the forms listed are considered the best fit to the general shape exhibited by the crystal in Fig. 1. No twinning was observed. The streak is white. Crystals are transparent with vitreous lustre. Monteneroite does not fluoresce under long- or shortwave ultraviolet light. Scratch tests indicated a Mohs hardness of ~ 2 . The mineral is somewhat sectile and crystals exhibit two cleavages, $\{010\}$ perfect and $\{001\}$ fair, and irregular stepped fracture. The density measured by flotation in a mixture of methylene iodide and toluene is $2.97(2)$ g cm $^{-3}$. The calculated density is 2.983 g cm $^{-3}$ for the empirical formula and 2.988 g cm $^{-3}$ for the ideal formula. Monteneroite crystals dissolve rapidly in dilute HCl at room temperature.

Monteneroite is optically biaxial (+), with the indices of refraction $\alpha = 1.604(2)$, $\beta = 1.637(2)$ and $\gamma = 1.688(2)$, determined in white light. The $2V$ is $80(1)^\circ$ measured directly on a spindle stage; the calculated $2V$ is 79.8° . The dispersion is $r < v$ slight and the optical orientation is $X = \mathbf{b}$, $Z \wedge \mathbf{c} = 52^\circ$ in the obtuse angle β . No pleochroism was observed. The Gladstone–Dale compatibility index, $1 - (K_p/K_c)$, is -0.003 for the empirical formula, in the range of superior compatibility (Mandarino, 2007).

Table 1. Electron microprobe analytical data (in wt.%) for monteneroite.

Constituent	Mean	Min.	Max.	S.D.	Probe standard
CuO	11.97	11.50	13.10	0.59	Cu metal
MnO	25.57	24.81	26.70	0.74	Rhodonite
As ₂ O ₅	39.30	38.43	40.24	0.74	Synthetic GaAs
H ₂ O*	24.56				
Total	101.40				

* Based on the structure; S.D. – standard deviation.

Raman spectroscopy

The Raman spectrum was obtained using a micro/macro Jobin Yvon LabRam HRVIS, equipped with a motorised x–y stage and an Olympus microscope. The back-scattered Raman signal was collected with a 50× objective and the spectrum was obtained from a randomly oriented crystal. The 632.8 nm line of a He–Ne laser was used as excitation; laser power was controlled by means of a series of density filters. The minimum lateral and depth resolution was set to a few μm. The system was calibrated using the 520.6 cm⁻¹ Raman band of silicon. The spectrum was collected

with multiple acquisitions and processed using *LabSpec 5* software. The spectrum from 4000 to 100 cm⁻¹ is shown in Fig. 3.

The Raman spectrum of monteneroite is dominated by the stretching and bending vibrations of AsO₄ tetrahedra and O–H stretching vibrations. The very broad band of relatively low intensity in the range ~3600 to ~2900 cm⁻¹ is attributed to the stretching O–H vibrations of molecular H₂O. According to the empirical correlation of Libowitzky (1999), the H···O_A lengths of the corresponding hydrogen bonds are in the range 2.7 to 1.7 Å, which is in line with the structure analysis. There are barely perceptible bands at ~1658 and ~1608 cm⁻¹, which can be ascribed to the ν₂ (δ) H–O–H deformation vibrations of molecular H₂O. The overlapping composite band of highest intensity, composed of bands at 898, 880, 866 (100% rel. int.) and 812 cm⁻¹, is attributed to overlapping ν₃ antisymmetric and ν₁ symmetric As–O vibrations of the AsO₄ tetrahedron. The bands of low intensity at ~468, 449, 435 and 428 cm⁻¹ are related to the ν₄ (δ) AsO₄ vibrations. At least two of the overlapping bands of medium–weak intensity at 435 and 428 cm⁻¹ are related to the ν₂ (δ) AsO₄ bending vibrations. The composite band at ~380 and 370 cm⁻¹ may be related to the stretching vibrations of the M1 and M2 octahedra.

Table 2. Powder X-ray data (*d* in Å) for monteneroite. Only calculated lines with *I* ≥ 1.5 are listed.

<i>l</i> _{obs}	<i>l</i> _{calc}	<i>d</i> _{obs}	<i>d</i> _{calc}	<i>hkl</i>
38	23	8.08	8.0619	1 1 0
100	100	6.86	6.8565	0 2 0
13	5	4.972	4.9830	2 0 0
	2		4.6546	0 0 1
50	21	4.507	4.4872	1̄ 1 1
10	4	4.139	4.1548	1 3 0
	3		4.0309	2 2 0
32	13	3.992	3.9945	2̄ 0 1
16	6	3.687	3.6906	1 1 1
	2		3.4515	2̄ 2 1
	3		3.4283	0 4 0
75	39, 10	3.287	3.2932, 3.2286	1̄ 3 1, 3 1 0
94	20, 23	3.032	3.0649, 3.0126	3̄ 1 1, 2 0 1
9	6	2.806	2.8244	2 4 0
88	19, 25	2.751	2.7603, 2.7581	0 4 1, 2 2 1
21	16	2.662	2.6873	3 3 0
8	9	2.591	2.6015	2̄ 4 1
26	17	2.500	2.5021	4 0 1
44	5, 18, 6	2.372	2.3819, 2.3750, 2.3505	1̄ 1 2, 1̄ 5 1, 4̄ 2 1
	2		2.2855	0 6 0
18	2, 6, 3	2.245	2.2630, 2.2436, 2.2302	2 4 1, 2̄ 2 2, 1 5 1
26	14	2.113	2.1150	3 5 0
	2		2.0515	0 6 1
	3		2.0210	4̄ 4 1
20	2, 5, 2, 4	1.996	1.9972, 1.9927, 1.9837, 1.9725	4̄ 0 2, 3̄ 3 2, 2̄ 6 1, 5 1 0
35	11	1.9381	1.9378	1 3 2
	2		1.9160	2 0 2
4	4	1.8660	1.8688	5 3 1
3	3	1.8121	1.8110	1̄ 7 1
28	3, 6, 9	1.7198	1.7257, 1.7228, 1.7141	4̄ 4 2, 3̄ 5 2, 0 8 0
29	12	1.6844	1.6869	1 5 2
	2		1.6725	2 4 2
19	4, 2, 5	1.6518	1.6610, 1.6543, 1.6409	6 0 0, 5̄ 3 2, 5 5 1
7	3	1.6163	1.6143	6 2 0
	2		1.5752	2̄ 8 1
24	4, 4, 2	1.5668	1.5722, 1.5711, 1.5515	6̄ 0 2, 5 3 1, 0 0 3
17	4, 2	1.5313	1.5386, 1.5325	6 4 1, 6 2 2
35	2, 2, 5, 2, 6	1.5026	1.5133, 1.5115, 1.5063, 1.4957, 1.4898	0 2 3, 1̄ 3 3, 4 0 2, 3̄ 3 3, 2 8 1
19	2, 3, 2	1.4637	1.4712, 1.4594, 1.4448	4 2 2, 2̄ 4 3, 1 7 2
18	3, 3, 2	1.4178	1.4283, 1.4141, 1.4135	5 5 1, 4̄ 8 1, 0 4 3
21	2, 7	1.3758	1.3830, 1.3713	1̄ 5 3, 0 10 0

The strongest lines are given in bold

Table 3. Data collection and structure refinement details for monteneroite.

Crystal data	
Structural formula	$(\text{Cu}_{0.69}\text{Mn}_{0.31})\text{Mn}_2^{2+}(\text{AsO}_4)_2 \cdot 8\text{H}_2\text{O}$
Space group	$C2/m$
Unit-cell dimensions	
a, b, c (Å)	10.3673(14), 13.713(2), 4.8420(8)
β (°)	105.992(8)
V (Å ³)	661.72(18)
Z	2
Density (calculated) (g cm ⁻³)	2.975
Absorption coefficient (mm ⁻¹)	8.324
$F(000)$	575.6
Crystal size (µm)	90 × 90 × 20
θ range for data collection (°)	4.09 to 25.01
Index ranges	$-11 \leq h \leq 11, -16 \leq k \leq 16, -5 \leq l \leq 5$
Data collection	
Diffractometer	Rigaku R-Axis Rapid II
X-ray radiation / power	MoK α ($\lambda = 0.71075$ Å)/50 kV, 40 mA
Temperature (K)	293(2)
Reflections collected	2116
Independent reflections	590 [$R_{\text{int}} = 0.050$]
Reflections with $I_o > 2\sigma I$	534
Completeness to $\theta = 25.01^\circ$	95.6%
Refinement	
Refinement method	Full-matrix least-squares on F^2
Parameters / restraints	69 / 6
Goodness-of-fit on F^2	1.096
Final R indices [$I > 2\sigma(I)$]	$R_1 = 0.0535, wR_2 = 0.1592$
R indices (all data)	$R_1 = 0.0569, wR_2 = 0.1646$
$\Delta\rho_{\text{max}}, \Delta\rho_{\text{min}}$ (e ⁻ /Å ³)	1.19 and -2.37

$R_{\text{int}} = \sum [F_o^2 - F_c^2(\text{mean})] / \sum [F_o^2]$. $\text{GoF} = S = \{ \sum [w(F_o^2 - F_c^2)^2] / (n-p) \}^{1/2}$. $R_1 = \sum ||F_o| - |F_c|| / \sum |F_o|$. $wR_2 = \{ \sum [w(F_o^2 - F_c^2)^2] / \sum [w(F_o^2)^2] \}^{1/2}$; $w = 1 / [\sigma^2(F_o^2) + (aP)^2 + bP]$ where a is 0.123, b is 3.000 and P is $[2F_c^2 + \text{Max}(F_o^2, 0)] / 3$.

There are numerous low-energy overlapping bands (348, 340, 317, 304, 270, 259, 240, 226, 192, 146 and 112 cm⁻¹) that are related to various $M\text{-O}_x$ stretching vibrations, deformations and phonons.

Chemical composition

Analyses of monteneroite (7 points on 5 crystal fragments) were done at the University of Utah on a Cameca SX-50 electron microprobe with four wavelength dispersive spectrometers using *Probe for EPMA* software. Analytical conditions were 15 kV accelerating voltage, 20 nA beam current and beam diameter of 10 µm. Raw X-ray intensities were corrected for matrix effects with a $\phi\rho(z)$ algorithm (Pouchou and Pichoir, 1991). There was significant beam damage during the analyses. Super-exponential time-dependent X-ray intensity corrections were applied for significant

'grow in' on all three elements. Insufficient material is available for a direct determination of H₂O, so it was calculated based on the structure. The high analytical total is probably due to H₂O loss under vacuum or during the analyses. Analytical data are given in Table 1.

The empirical formula (based on 16 O atoms per formula unit) is $\text{Cu}_{0.88}\text{Mn}_{2.11}\text{As}_{2.00}\text{O}_{16}\text{H}_{15.99}$ or formulated in accord with the structure, $(\text{Cu}_{0.88}\text{Mn}_{0.11})_{\Sigma 0.99}\text{Mn}_{2.00}^{2+}(\text{As}_{1.00}\text{O}_4)_2 \cdot 8\text{H}_2\text{O}$. The simplified formula is $(\text{Cu}^{2+}, \text{Mn}^{2+})\text{Mn}_2^{2+}(\text{AsO}_4)_2 \cdot 8\text{H}_2\text{O}$. The ideal formula is $\text{Cu}^{2+}\text{Mn}_2^{2+}(\text{AsO}_4)_2 \cdot 8\text{H}_2\text{O}$, which requires CuO 13.36, MnO 23.83, As₂O₅ 38.60, H₂O 24.21, total 100 wt.%.

X-ray crystallography and structure determination

Powder X-ray diffraction data were obtained on a Rigaku R-Axis Rapid II curved imaging plate microdiffractometer utilising monochromatised MoK α radiation. Observed d values and intensities were derived by profile fitting using *JADE Pro* software (Materials Data, Inc.). The observed powder data fit well with those calculated from the structure, also using *JADE Pro* (Table 2). The unit-cell parameters refined from the powder data using *JADE Pro* with whole-pattern fitting are: $a = 10.301(8)$, $b = 13.667(8)$, $c = 4.824(8)$ Å, $\beta = 106.076(19)^\circ$ and $V = 652.6(13)$ Å³.

Single-crystal X-ray studies were carried out using the same diffractometer and radiation noted above. The Rigaku *CrystalClear* software package was used for processing the structure data, including the application of an empirical multi-scan absorption correction using *ABSCOR* (Higashi, 2001). The structure was solved using *SHELXT* (Sheldrick, 2015a). Refinement proceeded by full-matrix least-squares on F^2 using *SHELXL-2016* (Sheldrick, 2015b). The occupancies of the two octahedrally coordinated cation sites were refined. The $M2$ site was shown to be fully occupied by Mn, while the $M1$ site was refined to a joint occupancy of $\text{Cu}_{0.69}\text{Mn}_{0.31}$. All non-hydrogen sites were refined with anisotropic displacement parameters. Difference-Fourier syntheses located all H atom positions, which were then refined with soft restraints of 0.82(3) Å on the O-H distances and 1.30(3) Å on the H-H distances, and with the U_{eq} of each H set to $\times 1.2$ that of its donor O atom. Data collection and refinement details are given in Table 3, atom coordinates and displacement parameters in Table 4, selected bond distances in Table 5 and a bond-valence analysis in Table 6. The crystallographic information files have been deposited with the Principal Editor of *Mineralogical Magazine* and are available as Supplementary material (see below).

Table 4. Atom positions and displacement parameters (Å²) for monteneroite.

	x/a	y/b	z/c	U_{eq}	U^{11}	U^{22}	U^{33}	U^{23}	U^{13}	U^{12}
Cu(M1)*	1/2	0	1/2	0.0218(9)	0.0285(14)	0.0241(13)	0.0129(12)	0	0.0059(8)	0
Mn(M2)	0	0.11564(11)	1/2	0.0241(7)	0.0369(12)	0.0222(11)	0.0146(9)	0	0.0091(7)	0
As	0.18938(10)	0	0.1301(2)	0.0221(6)	0.0315(9)	0.0234(8)	0.0125(8)	0	0.0077(6)	0
O1	0.3539(7)	0	0.1365(14)	0.0246(17)	0.022(4)	0.036(4)	0.016(3)	0	0.005(3)	0
O2	0.1622(6)	0.1034(4)	0.2890(11)	0.0266(13)	0.043(3)	0.024(3)	0.017(3)	0.000(2)	0.016(2)	0.002(2)
O3	0.1012(8)	0	-0.2171(15)	0.0258(17)	0.039(4)	0.022(4)	0.015(3)	0	0.005(3)	0
O4	0.4020(7)	0.1143(5)	0.6980(13)	0.0407(16)	0.044(4)	0.052(4)	0.022(3)	0.008(3)	0.004(3)	-0.008(3)
H4A	0.382(10)	0.106(8)	0.846(12)	0.049						
H4B	0.335(6)	0.121(8)	0.573(14)	0.049						
O5	0.1019(7)	0.2286(4)	0.7954(12)	0.0376(15)	0.053(4)	0.035(3)	0.026(3)	-0.007(3)	0.013(3)	-0.005(3)
H5A	0.087(10)	0.287(3)	0.795(17)	0.045						
H5B	0.127(11)	0.211(6)	0.961(9)	0.045						

*Occupancy $\text{Cu}_{0.69}\text{Mn}_{0.31(5)}$

Table 5. Selected interatomic distances (Å), angles (°) and distortion measures of polyhedra in monteneroite.

<i>M1</i>		<i>M2</i>			
Cu–O1 ×2	1.981(7)	Mn–O3 ×2	2.168(5)	As–O2 ×2	1.674(5)
Cu–O4 ×4	2.223(7)	Mn–O5 ×2	2.175(6)	As–O3	1.678(7)
<Cu–O>	2.142	Mn–O2 ×2	2.201(5)	As–O1	1.697(7)
		<Mn–O>	2.181	<As–O>	1.681
<i>ECoN</i>	5.079	<i>ECoN</i>	5.991		
Δ	0.050	Δ	0.006		
Hydrogen bonds lengths (Å) and angles (°)					
<i>D–H...A</i>	<i>D–H</i>	<i>H...A</i>	<i>D...A</i>	< <i>DHA</i>	
O4–H4A...O1	0.80(3)	2.10(7)	2.792(8)	145(10)	
O4–H4B...O2	0.79(3)	1.95(4)	2.722(9)	165(11)	
O5–H5A...O4	0.81(3)	2.29(7)	2.936(9)	137(9)	
O5–H5B...O2	0.81(3)	2.12(4)	2.868(8)	153(8)	

ECoN – effective coordination number defined by Hoppe (1979); Δ – distortion index defined after Baur (1974); *D* – donor; *A* – acceptor.

Table 6. Bond-valences analysis for monteneroite. Values are in valence units (vu).

	Cu (<i>M1</i>)	Mn (<i>M2</i>)	As	H bonds	Σ
O1	0.48 ^{×2↓}		1.21	0.19	1.88
O2		0.33 ^{×2↓}	1.30 ^{×2↓}	0.22, 0.16	2.01
O3		0.36 ^{×2↓→}	1.28		2.00
O4	0.22 ^{×4↓}			–0.19, –0.22, 0.14	–0.05
O5		0.35 ^{×2↓}		–0.14, –0.16	0.05
Σ	1.94	2.08	5.09		

Multiplicities indicated by ×↓→. The bond valences for the Cu site are based on its refined joint occupancy. Bond-valence parameters are from Gagné and Hawthorne (2015). Hydrogen-bond strengths are based on O–O distances according to the relation of Ferraris and Ivaldi (1988).

Description of the structure

Monteneroite is isostructural with other minerals with vivianite-type structures. Vivianite-type structures consist of $M\text{IO}_2(\text{H}_2\text{O})_4$ octahedra and $M_2\text{O}_6(\text{H}_2\text{O})_4$ edge-sharing octahedral dimers that are linked via XO_4 tetrahedra (where $X = \text{P}$ or As) and hydrogen bonds to form layers parallel to {010} (Fig. 4). Adjacent layers are linked by hydrogen bonds only (Fig. 5). The coordinations of the *M1* and *M2* sites, while both octahedral, are significantly different. Several investigations for Mg-bearing vivianite-structure-type phases have shown partial ordering of cations between the *M1* and *M2* sites and, as noted above, baričite was shown by Yakubovich *et al.* (2001) to have Fe dominant in the *M1* site and Mg dominant in the *M2* site; however, for those phases in which the principal cations are Co, Zn, Ni or Cu, site ordering has not been shown conclusively, possibly because of the similarities in scattering powers of these cations (see Plášil *et al.*, 2017, and references therein).

The coordination geometries of the *M1* and *M2* sites in the structure of monteneroite differ more markedly than those in other minerals with vivianite-type structures. While the average bond lengths of the sites are similar, 2.142 and 2.181 Å, respectively, the *M1* site is much more strongly distorted (see Table 5). The *M1* site exhibits a compressed Jahn–Teller distortion with short apical bonds of 1.981(7) Å and long equatorial bonds of 2.223(7) Å. In contrast, the *M2* site has a much narrower range of bond lengths (2.168–2.201 Å). Comparisons of the differences in the coordinations for the *M1* and *M2* sites are provided by the

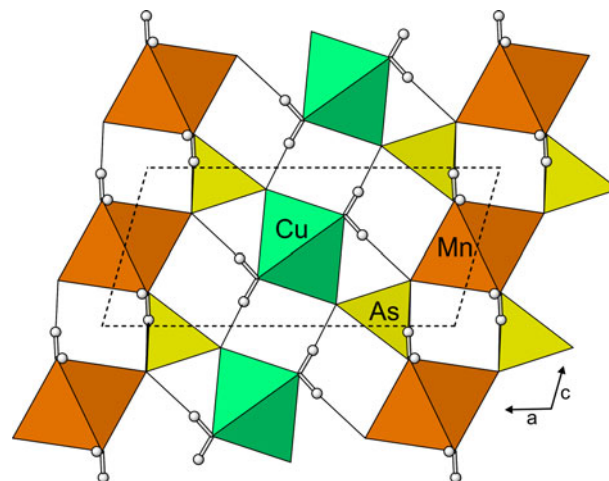


Fig. 4. Layer composed of $\text{CuO}_2(\text{H}_2\text{O})_4$ octahedra, $\text{Mn}_2\text{O}_6(\text{H}_2\text{O})_4$ octahedral dimers (two octahedra superimposed) and AsO_4 tetrahedra in the structure of monteneroite. Hydrogen bonds are shown as thin black lines. The view is down [010] and the unit cell outline is shown with dashed lines.

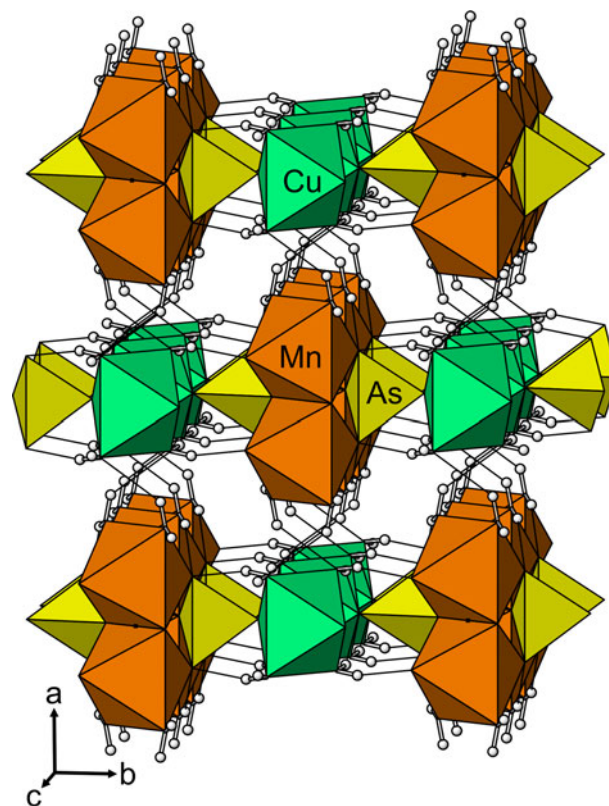


Fig. 5. Stacking of polyhedral layers in the structure of monteneroite. Hydrogen bonds are shown as thin black lines. The view is slightly canted along [001].

effective coordination number (*ECoN*) defined by Hoppe (1979) and the distortion index (Δ) after Baur (1974). The *ECoN* values for *M1* and *M2* are 5.079 and 5.991, respectively; the Δ values are 0.050 and 0.006, respectively (see Table 5).

Besides the strong ordering of Cu and Mn indicated by the refinements (BVS) at these sites, the ordering is also supported by bond-valence summations (BVS) at these sites. The *M1* site has a BVS of 1.76 valence units (vu) with occupancy only by Cu^{2+} and 2.38 vu with only Mn^{2+} . Based on the refined *M1* occupancy

Table 7. Arsenate minerals with the vivianite structure.

Mineral Type locality	Monteneroite Monte Nero, Italy	Babánekite Jáchymov, CZ	Erythrite Schneeberg, Germany	Annabergite Annaberg, Germany	Hörnesite Banat, Hungary	Manganohörnesite Långban, Sweden	Köttigite Schneeberg, Germany	Parasymplesite Kiura Mine, Japan
M^{2+} (ideal.)	CuMn ₂	Cu ₃	Co ₃	Ni ₃	Mg ₃	(Mn,Mg) ₃	Zn ₃	Fe ₃
M^{2+} (meas.)	Cu _{0.88} Mn _{2.11}	(Cu _{1.12} Zn _{0.78} Co _{0.69} Ni _{0.32})	(Co _{2.01} Fe _{0.74} Ni _{0.25})	(Ni _{2.48} Mg _{0.50} Fe _{0.02})	–	(Mn _{1.65} Mg _{1.32})	(Zn _{2.44} Co _{0.42} Ni _{0.14})	–
Space group	C2/m	C2/m	C2/m	C2/m	C2/m	P2 ₁ /c	C2/m	C2/m
<i>a</i> (Å)	10.3673(14)	10.1729(3)	10.251(3)	10.179(2)	10.137(2)	10.38	10.241(3)	10.276(4)
<i>b</i> (Å)	13.713(2)	13.5088(4)	13.447(4)	13.309(3)	13.445(2)	28.09	13.405(3)	13.480(5)
<i>c</i> (Å)	4.8420(8)	4.7496(1)	4.764(1)	4.725(1)	4.754(1)	4.774	4.757(2)	4.771(2)
β (°)	105.922(8)	105.399(2)	104.98(1)	105.00(1)	101.73(2)	105.7	105.21(2)	105.02(5)
<i>V</i> (Å ³)	661.72(18)	629.28(3)	634.4	618.2	634.17	1340.04	630.2(2)	–
<i>Z</i>	2	2	2	2	2	4	2	2
Strongest lines in	6.86/100 4.507/50	6.743/100 7.936/11	6.65/100 7.89/6	6.58/100 7.82/25	8.55/10 5.11/5	8.19 (80) 7.01 (100)	7.95 (37) 6.70 (100)	7.91 (70) 6.68 (100)
PXRD	3.287/75	3.23/14	3.34/8	4.33/20	4.30/6	3.25 (60)	3.22 (39)	4.41 (40)
[<i>d</i> (in Å) / <i>l</i>]	3.032/94 2.751/88	2.715/11 1.686/16	3.22/12 2.70/8	3.18/26 2.98/30	3.59/9 3.45/4	3.09 (60) 3.02 (70)	2.99 (28) 2.73 (26)	3.91 (30) 3.24 (50)
Optical data	Biaxial (+)		Biaxial (+)	Biaxial (+)	Biaxial (+)	Biaxial (+)	Biaxial (+)	Biaxial (+)
α	1.604(2)		1.622–1.629	1.622	1.563	1.579	1.619–1.622	1.620–1.628
β (n_{calc})	1.637(2)	1.662	1.660–1.663	1.658	1.571	1.589	1.638–1.645	1.648–1.660
γ	1.688(2)		1.681–1.701	1.687	1.596	1.609	1.671–1.681	1.685–1.705
2 <i>V</i> (°)	79.8°		up to 90°	84°	65°	65–70°	74–85°	86°
Reference	Current study	Plášil <i>et al.</i> (2017)	Wildner <i>et al.</i> (1996)	Wildner <i>et al.</i> (1996)	Palache <i>et al.</i> (1951)	Gabrielson (1954)	Dana (1850)	Ito <i>et al.</i> (1954)

M^{2+} indicates both octahedral cation sites in the structure.

The unit-cell parameters for hörnesite are from Jambor and Dutrizac (1995).

The M^{2+} measured value for köttigite and the unit-cell parameters for parasymplesite are from Sturman (1976).

The strongest powder X-ray diffraction lines for köttigite are calculated from the crystal structure of Hill (1979).

The optical properties for babánekite, erythrite, annabergite, hörnesite, manganohörnesite and parasymplesite are from Anthony *et al.* (1990).

($\text{Cu}_{0.69}\text{Mn}_{0.31}^{2+}$), the BVS is 1.94 vu. The M2 site has a BVS of 2.08 vu with only Mn^{2+} , but a BVS of 1.49 vu with only Cu^{2+} .

Monteneroite is an ordered intermediate between manganohörsnesite (Gabrielson, 1954), $\text{Mn}_3^{2+}(\text{AsO}_4)_2 \cdot 8\text{H}_2\text{O}$ and babánekite (Plášil *et al.*, 2017), $\text{Cu}_3^{2+}(\text{AsO}_4)_2 \cdot 8\text{H}_2\text{O}$. Selected data for arsenate minerals with the vivianite structure are compared in Table 7. The vivianite group has not yet been formally approved by the CNMNC; however, a vivianite-group proposal is in preparation.

Supplementary material. To view supplementary material for this article, please visit <https://doi.org/10.1180/mgm.2020.76>

Acknowledgements. Anonymous reviewers are thanked for their constructive comments. A portion of this study was funded by the John Jago Trelawney Endowment to the Mineral Sciences Department of the Natural History Museum of Los Angeles County and by the by the Czech Science Foundation (GACR 17-09161S) to J.P.

References

- Anthony J.W., Bideaux R.A., Bladh K.W. and Nichols M.C. (1990) *Handbook of Mineralogy IV, Arsenates, Phosphates, Vanadates*. Mineral Data Publishing, Tucson, Arizona, pp 1–680.
- Baur W.H. (1974) The geometry of polyhedral distortions. Predictive relationships for the phosphate group. *Acta Crystallographica*, **B30**, 1195–1215.
- Callegari A.M., Boiocchi M., Ciriotti M. and Balestra C. (2012) Coralloite, $\text{Mn}^{2+}\text{Mn}^{3+}(\text{AsO}_4)_2(\text{OH})_2 \cdot 4\text{H}_2\text{O}$, a new mixed valence Mn hydrate arsenate: Crystal structure and relationships with bermanite and whitmoreite mineral groups. *American Mineralogist*, **97**, 727–734.
- Dana J.D. (1850) Köttigite. Pp. 487 in: *A System of Mineralogy*, 3rd Edition. George P. Putnam, New York and London.
- Ferraris G. and Ivaldi G. (1988) Bond valence vs. bond length in O...O hydrogen bonds. *Acta Crystallographica*, **B44**, 341–344.
- Gabrielson O. (1954) Manganiferous hoernesite and manganese-hoernesite from Långban, Sweden. *Arkiv för Mineralogi och Geologi*, **1**, 333–337.
- Gagné O.C. and Hawthorne F.C. (2015) Comprehensive derivation of bond-valence parameters for ion pairs involving oxygen. *Acta Crystallographica*, **B71**, 562–578.
- Higashi T. (2001) *ABSCOR*. Rigaku Corporation, Tokyo.
- Hill R.J. (1979) The crystal structure of köttigite. *American Mineralogist*, **64**, 376–382.
- Hoppe R. (1979) Effective coordination number (ECoN) and mean-fictive ionic radii (Mefir). *Zeitschrift für Kristallographie*, **150**, 23–52.
- Ito T., Minato H. and Sakurai K. (1954) Parasymplectite, a new mineral polymorphous with symplectite. *Proceedings of the Japan Academy*, **30**, 318–324.
- Jambor J.L. and Dutrizac J.E. (1995) Solid solutions in annabergite–erythrite–hörsnesite synthetic system. *The Canadian Mineralogist*, **33**, 1063–1071.
- Kampf A.R., Cámara F., Ciriotti M.E., Nash B.P., Balestra C. and Chiappino L. (2016) Castellaroite, $\text{Mn}_3^{2+}(\text{AsO}_4)_2 \cdot 4.5\text{H}_2\text{O}$, a new mineral from Italy related to metaswitzerite. *European Journal of Mineralogy*, **28**, 687–696.
- Kampf A.R., Plášil J., Nash B.P., Ciriotti M.E., Castellano F. and Chiappino L. (2020) Monteneroite, IMA 2020-028. CNMNC Newsletter No. 56; *Mineralogical Magazine*, **84**, 623–627.
- Libowitzky E. (1999) Correlation of O–H stretching frequencies and O–H...O hydrogen bond lengths in minerals. *Monatshefte für Chemie*, **130**, 1047–1059.
- Mandarino J.A. (2007) The Gladstone–Dale compatibility of minerals and its use in selecting mineral species for further study. *The Canadian Mineralogist*, **45**, 1307–1324.
- Marescotti P. and Cabella R. (1996) Significance of chemical variations in a chert sequence of the “Diaspri di Monte Alpe” formation (Val Graveglia, northern Apennine, Italy). *Ofolit*, **21**, 139–144.
- Palache C., Berman H. and Frondel C. (1951) *The System of Mineralogy of James Dwight Dana and Edward Salisbury Dana, Yale University 1837–1892, Volume II. Halides, Nitrates, Borates, Carbonates, Sulfates, Phosphates, Arsenates, Tungstates, Molybdates, etc.* John Wiley & Sons, New York, pp. 1–755.
- Plášil J., Škácha P., Sejkora J., Škoda R., Novák M., Veselovský F. and Hloušek J. (2017) Babánekite, $\text{Cu}_3(\text{AsO}_4)_2 \cdot 8\text{H}_2\text{O}$, from Jachymov, Czech Republic – a new member of the vivianite group. *Journal of Geosciences*, **62**, 261–270.
- Pouchou J.-L. and Pichoir F. (1991) Quantitative analysis of homogeneous or stratified microvolumes applying the model “PAP.” Pp. 31–75 in: *Electron Probe Quantitation* (K.F.J. Heinrich and D.E. Newbury, editors). Plenum Press, New York.
- Sheldrick G.M. (2015a) SHELXT – Integrated space-group and crystal-structure determination. *Acta Crystallographica*, **A71**, 3–8.
- Sheldrick G.M. (2015b) Crystal structure refinement with SHELX. *Acta Crystallographica*, **C71**, 3–8.
- Sturman B.D. (1976) New data for köttigite and parasymplectite. *The Canadian Mineralogist*, **14**, 437–441.
- Wildner M., Giester G., Lengauer C.L. and McCammon C.A. (1996) Structure and crystal chemistry of vivianite-type compounds: crystal structures of erythrite and annabergite with a Mössbauer study of erythrite. *European Journal of Mineralogy*, **8**, 187–192.
- Yakubovich O.V., Massa W., Liferovich R.P. and McCammon C.A. (2001) The crystal structure of baričite, $(\text{Mg}_{1.70}\text{Fe}_{1.30})(\text{PO}_4)_2 \cdot 8\text{H}_2\text{O}$, the magnesium-dominant member of the vivianite group. *The Canadian Mineralogist*, **39**, 1317–1324.